

Attitude Stability of tilt-rotor UAV during Obstacle Avoidance and Transition mode

Mingyu Ren^{1,*},

Jiacheng Tian²,

Yuxuan Li³

¹Mechanical Engineering, Dalian University of Technology, Dalian, 116024, China, 17709846725@163.com

²Mechanical Engineering, Dalian University of Technology, Dalian, 116024, China, tianjiacheng@mail.dlut.edu.cn

³United World College South East Asia Dover, Singapore, 139654, Singapore, noobflipx1@gmail.com

*Corresponding author email: 17709846725@163.com

Abstract:

This paper presents a comprehensive study focused on the optimization and enhancement of the control system for tilt-rotor Unmanned Aerial Vehicles (UAVs) during the critical transition phase. We have developed a two-dimensional system dynamics model of the tilt-rotor UAV and utilized Simulink simulations to analyze and refine the control strategies. Specifically, we have implemented Proportional-Integral-Derivative (PID) controllers to stabilize the UAV, while employing Genetic Algorithm (GA) techniques to optimize the trajectory of the UAV.

Keywords: UAV; tilt-rotor; Transition flight; PID controller; Genetic Algorithm (GA); trajectory optimization; flight simulation

1. Introduction

Unmanned Aerial Vehicles (UAV) have gained significant attention in recent years due to their versatility and potential applications across various industries. The tilt-rotor UAV, as a hybrid design, combines the advantages of both fixed-wing and rotor craft platforms, offering the unique capability of transitioning between vertical takeoff and landing (VTOL) and high-speed, long-range flight[1-5]. This versatility enhances operational flexibility and flight efficiency, making tilt-rotor UAV an attractive choice for various missions.

However, the control of tilt-rotor UAVs during the transition phase from fixed-wing to rotor mode pres-

ents significant challenges due to abrupt changes in aerodynamic characteristics, strong coupling of control inputs, and unstable dynamic responses [6]. Recent research has made progress in addressing these challenges. One notable contribution is the paper [1], which thoroughly analyzed the unique control requirements during the transition phase and proposed an innovative flight control system tailored specifically for tilt-rotor UAV. Through simulations, the authors rigorously validated the effectiveness of their design in improving control performance and facilitating smooth transitions. However, while this work represents a substantial advancement, its limitations lie in potential further refinement, particularly regarding stability performance under extreme flight

conditions or in the presence of unforeseen disturbances. It is difficult to avoid tilt-rotor UAV encountering narrow spaces and sudden interruptions when cruising at high speed in fixed-wing mode [11]. Even rapid interception will lead to loss of attitude. Paper [4] designed two controllers for fixed wing and quad copter respectively. Allocate control weight according to the tilt angle of the motor. This control idea performs well when converting from a quad copter to a fixed wing at low speeds. But when switching from fixed-wing mode to quad-rotor mode at high speed. The posture and speed of the UAV have undergone unstable oscillations and mutations.

Traditional control methods, struggle to fully cope with these nonlinear and time-varying dynamics, especially under extreme operating conditions. Therefore, developing an effective control strategy that can handle the complexity of the transition stage and optimize the UAV's trajectory is crucial [12].

This paper addresses these challenges by developing a comprehensive and efficient flight control system for tilt-rotor UAV. We start by creating a two-dimensional mathematical model of the UAV's dynamics, propulsion, and aerodynamics using MATLAB/Simulink [5]. This model serves as the basis for simulating the UAV's behavior and analyzing its control performance.

To refine the control system, we implement PID controllers and employ Genetic Algorithm (GA) optimization techniques. PID controllers are chosen for their simplicity

and robustness in controlling various dynamical systems. However, to achieve optimal performance, we utilize GA to optimize the UAV's trajectory, ensuring stability and efficiency during the transition phase[9].

The results of our simulations demonstrate a significant improvement in the control and transition efficiency of tilt-rotor UAV. Our findings contribute to the ongoing discourse on advancing UAV technologies towards greater efficiency, reliability, and environmental sustainability. By refining the attitude control of tilt-rotor UAV, we aim to contribute to the development of a new generation of UAV with enhanced capabilities and wider applications.

2. Method

2.1 Simulation environment and project content

Use Simulink/Matlab as the simulation environment. Use Solidworks to build the physical model; Considering that the main changes that occur to the aircraft in the deceleration state occur in the pitch angle and the speed changes on the X-axis and Y-axis, this model only studies the attitude and speed of the UAV in two-dimensional space [1-4]. Use Y3+ fixed wing as the basic configuration of the aircraft, in which the aircraft tilt angle can rotate from 0 to 270°.The three motors of this model can all rotate relative to the body coordinate system[7].

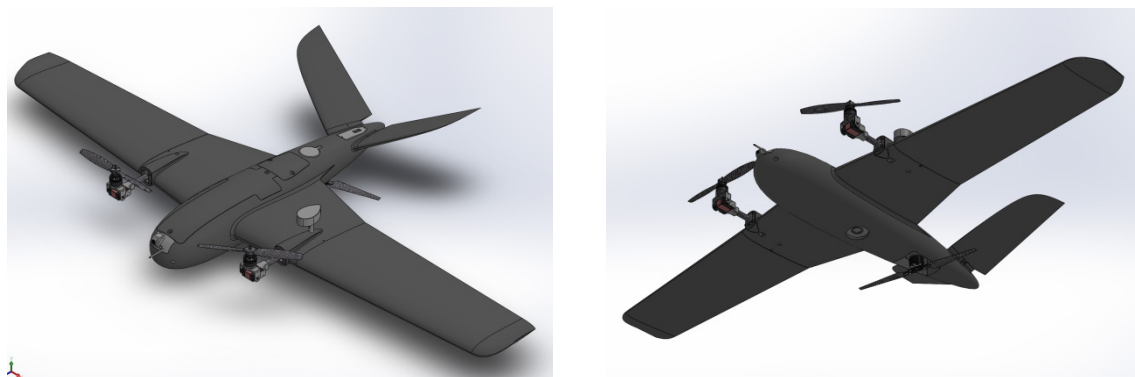


Fig.1 SolidWorks model

In this SW model, the back motor cannot rotate due to the lack of a servo, but the parameters are correct.

2.2 Dynamic Model

(1) Construct coordinate systems and vector labels[1-4][6][10]

Label	Content
n	World coordinate system
b	Body coordinate system
r, l, b, F, V	Motor and Fix wing coordinate system
α_1	Front Steering gear tilt angle

α_2	Back Steering gear tilt angle
$m=0.9839$ kg	Quality
$g=9.81$ m/ s^2	Gravity acceleration
$A_F=0.4349$ m^2	Total front fixed wing area
$A_V=0.0920$ m^2	Total back fixed wing area
$C_L=0.50$	Fixed wing lift parameters
$C_D=0.05$	Fixed wing drag parameters
$L_F=0.020$ m	Distance of front fixed wing to gravity center
$L_V=0.189$ m	Distance of back fixed wing to gravity center
$P_a=101.325$ kPa	Standard atmospheric pressure
$\rho=1$ kg / m^3	Standard atmospheric density
T_L	Front left motor lift
T_r	Front right motor lift
T_b	Back motor lift
$L_1=0.3577$ m	Distance of front motor to gravity center
$L_2=0.1832$ m	Distance of back motor to gravity center
θ	Angle
$\dot{\theta}$	Angular velocity
$\ddot{\theta}$	Angular Acceleration
x	X-position
y	Y-position
$\dot{x}=V$	X-axis speed
\dot{y}	Y-axis speed
\ddot{x}	X-acceleration
\ddot{y}	Y-acceleration
D	Propeller diameter
P	Screw pitch
C	Empirical coefficient
W	Propeller width
W_r	Propeller speed
C_b^n	Transition matrix(from b to n)
M	Resultant moment
F_x	Resultant force in Y direction in body coordinate system
F_y	Resultant force in Y direction in body coordinate system
F^n	Resultant force in the world coordinate system
$I=1$ kg * m^2	Moment of inertia
$\beta = \frac{\pi}{3}$ rad	Angle between back wing and body horizontal plane

$K_{p_1}, K_{d_1}, K_{p_2}, K_{d_2}, K_{p_3}, K_{d_3}$	PID parameter
Hyper parameters remain constant throughout the model	

(2) Forces and Moments

Rotor and fix wing lift:

$$T_r = D \cdot P \cdot W \cdot \left(\frac{W_r}{2\pi}\right)^2 \cdot P_a \cdot C; T_L = D \cdot P \cdot W \cdot \left(\frac{W_r}{2\pi}\right)^2 \cdot P_a \cdot C; T_b$$

$$= D \cdot P \cdot W \cdot \left(\frac{W_r}{2\pi}\right)^2 \cdot P_a \cdot C;$$

Rotor and fix wing lift to body frame:

Motor:

$$T_r^b = [T_r \sin \alpha_1 \quad T_r \cos \alpha_1]^T; \quad T_l^b = [T_l \sin \alpha_1 \quad T_l \cos \alpha_1]^T;$$

$$T_b^b = [T_b \sin \alpha_2 \quad T_b \cos \alpha_2]^T;$$

Fix wing:

$$F_{F_x} = -V^2 \cdot \rho \cdot A_F \cdot C_D; F_{F_y} = V^2 \cdot \rho \cdot A_F \cdot C_L;$$

$$F_{V_x} = -V^2 \cdot \rho \cdot A_V \cdot C_D; F_{V_y} = V^2 \cdot \rho \cdot A_V \cdot C_L \cos \beta;$$

$$F_F^b = [F_{F_x} \quad F_{F_y}]^T; F_V^b = [F_{V_x} \quad F_{V_y}]^T; G_n = [0 \quad -mg]^T;$$

Body frame to world frame:

$$C_b^n = \begin{bmatrix} \cos \theta & -\sin \theta \\ \sin \theta & \cos \theta \end{bmatrix};$$

$$F^n = C_b^n (T_r^b + T_l^b + T_b^b + F_F^b + F_V^b) + G_n;$$

Expanding this equation, we get

$$m \begin{bmatrix} \ddot{x} \\ \ddot{y} \end{bmatrix}$$

$$= \begin{bmatrix} \cos \theta & -\sin \theta \\ \sin \theta & \cos \theta \end{bmatrix} \begin{bmatrix} (T_r + T_l) \sin \alpha_1 + T_b \sin \alpha_2 + F_{F_x} + F_{V_x} \\ (T_r + T_l) \cos \alpha_1 + T_b \cos \alpha_2 + F_{F_y} + F_{V_y} \end{bmatrix}$$

$$+ \begin{bmatrix} 0 \\ -mg \end{bmatrix};$$

Acceleration:

$$m \cdot \ddot{x} = \cos \theta [(T_r + T_l) \sin \alpha_1 + T_b \sin \alpha_2 + F_{F_x} + F_{V_x}] -$$

$$\sin \theta [(T_r + T_l) \cos \alpha_1 + T_b \cos \alpha_2 + F_{F_y} + F_{V_y}];$$

$$m \cdot \ddot{y} = \sin \theta [(T_r + T_l) \sin \alpha_1 + T_b \sin \alpha_2 + F_{F_x} + F_{V_x}] - mg +$$

$$\cos \theta [(T_r + T_l) \cos \alpha_1 + T_b \cos \alpha_2 + F_{F_y} + F_{V_y}];$$

Angular Acceleration:

$$I \cdot \ddot{\theta} = T_r \cos \alpha_1 L_1 + T_l \cos \alpha_1 L_1 - T_b \sin \alpha_2 L_2 + L_F \cdot F_{F_y} - L_V \cdot F_{V_y};$$

for any condition $L_F F_{F_y} - L_V F_{V_y} = 0$, we get:

$$I \cdot \ddot{\theta} = T_r \cos \alpha_1 L_1 + T_l \cos \alpha_1 L_1 - T_b \sin \alpha_2 L_2;$$

Velocity and position:

$$x = \dot{x} \cdot dt; \quad V = \dot{x} \cdot \dot{x} \cdot dt; \quad y = \dot{y} \cdot dt; \quad \dot{y} = \ddot{y} \cdot dt; \quad \theta = \dot{\theta} \cdot dt; \quad \dot{\theta}$$

$$= \ddot{\theta} \cdot dt;$$

2.3 PD controller & QR control

(1) PD controller is used to control the stability of the attitude[8]:

Get the Moment:

$$M = K_{p_1} \cdot \theta + K_{d_1} \cdot \dot{\theta};$$

(2) Control changes in X-axis and Y-axis speed and displacement through PD controller

Get the values of F_x and F_y :

$$F_x = K_{p_2} \cdot x + K_{d_2} \cdot \dot{x}; \quad F_y = K_{p_3} \cdot y + K_{d_3} \cdot \dot{y};$$

(3) Get the value of $F_{x_1}, F_{x_2}, F_{y_1}, F_{y_2}$ through QR

Suppose $F_{x_1} \setminus \& F_{x_2}$ has no influence on the θ for they always in a line with gravity center,

So we can get $F_{y_1} \setminus \& F_{y_2}$ through:

$$M = F_{y_1} \cdot L_1 + F_{y_2} \cdot L_2;$$

$$F_y - F_{F_y} - F_{V_y} = F_{y_1} + F_{y_2};$$

$F_{x_1} \setminus \& F_{x_2}$ are under determined, so get through QR:

$$F_x - F_{F_x} - F_{V_x} = F_{x_1} + F_{x_2};$$

Limited:

$$F_{x_1}^2 + F_{x_2}^2 \leq 100;$$

Initial condition:

$$F_{x_1} = F_{x_2} = \frac{F_x}{2};$$

(4) ,Get α_1 & α_2 and T_L, T_r, T_b through $F_{x_1}, F_{x_2}, F_{y_1}, F_{y_2}$:

$$\alpha_1 = \arctan\left(\frac{F_{y_1}}{F_{x_1}}\right); \quad \alpha_2 = \arctan\left(\frac{F_{y_2}}{F_{x_2}}\right);$$

$$T_l = T_r = \frac{(F_{x_1}^2 + F_{y_1}^2)^{0.5}}{2}; \quad T_b = (F_{x_2}^2 + F_{y_2}^2)^{0.5};$$

2.4 Genetic Algorithm Trajectory optimization

Trajectory optimization is an important problem in robot navigation, path planning, aerospace and other fields. In complex environments, where there are multiple obstacles and certain boundary conditions, finding an optimal path from the starting point to the end point becomes particularly complex. As a powerful heuristic search algorithm,

genetic algorithm has been widely used in trajectory optimization because of its global search ability and robustness.

Genetic algorithm is a search algorithm that simulates the principles of natural selection and genetics. It simulates biological evolution by maintaining a population in which each individual represents a potential solution to a problem. The algorithm makes the population gradually evolve to a state containing better solutions through the operations of selection, crossover and mutation[9][13]. The fitness function is used to evaluate the pros and cons of each individual in the population. We take the length of the path, smoothness and distance from obstacles as factors affecting the fitness function.

When the algorithm reaches the maximum number of iterations, the algorithm stops. And after the last iteration,

the optimal solution set is selected for output. Instead of displaying an image of only one optimal solution, the program visualizes all non-dominant solutions. This is designed to demonstrate the diversity of algorithms and a variety of options, or for subsequent analysis and comparison.

2.5 GA + Controller

Using the optimal route planned by GA as the control route, the tilt rotor maintains its attitude stability while performing mode conversion in obstacle avoidance flight[9][13].

3. Result

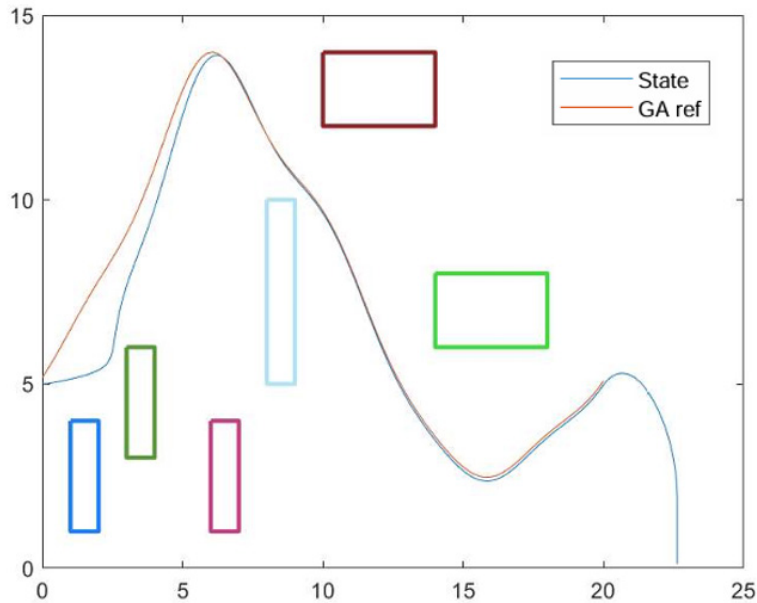


Fig.2 Flight trajectory and desired trajectory

The initial state of tilt-rotor UAV flight

is $[x_0, y_0, \theta_0, \dot{x}_0, \dot{y}_0, \dot{\theta}_0]$, and its value is set

to $[0, 5, 0, 10, 0, 0]$. The system simulation results are shown in the figure.

UAV successfully achieved a complex obstacle avoidance

task while maintaining a high speed flight state ($V=10$), followed by a smooth transition to the landing phase. In this process, the trajectory control of the UAV maintains a high degree of consistency with the original set trajectory, which fully verifies its accurate path planning ability and the stability of the flight control system.

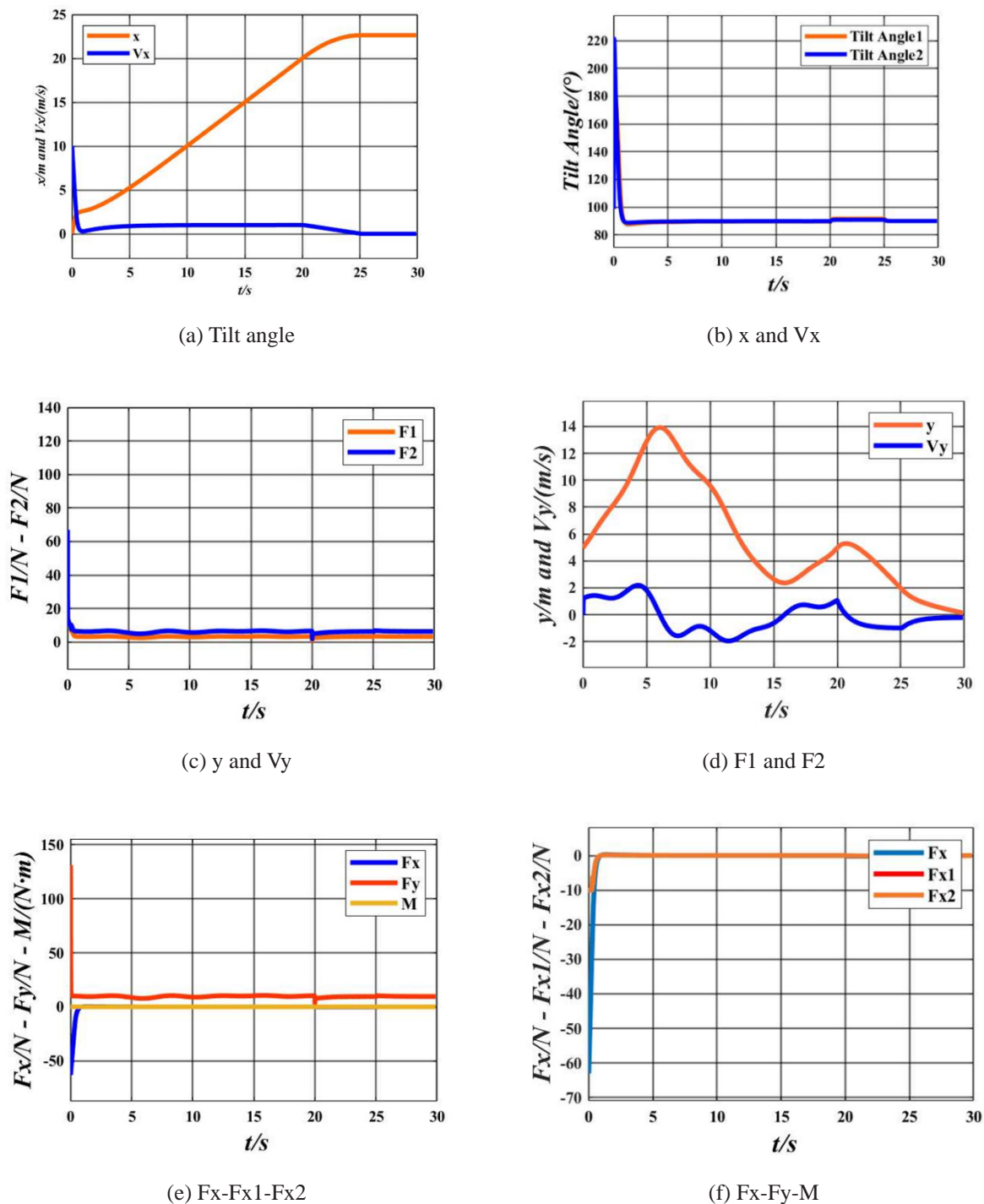


Fig.3 Simulation Results

In the obstacle avoidance process, see the Fig.2, the UAV identifies and avoids preset obstacles through genetic algorithms. This not only demonstrates the UAV's ability to respond flexibly in complex environments, but also proves the effectiveness and reliability of its flight control algorithm in handling unexpected situations. In addition, the posture of the drone remained stable during the obstacle

avoidance process without any drastic fluctuations or out-of-control phenomena, further highlighting its high-performance flight control system. See Fig.3(a) & Fig.3(d) & Fig.3(e) & Fig.3(f) tilt angle and lift is a continuous function with time, which is controllable.

During the transition to the landing phase, the drone also demonstrated excellent control. By precisely adjusting

flight parameters and attitude, the UAV successfully completed a smooth transition from high-speed flight to low-speed landing. In this process, the trajectory control and pose stability of the UAV meet the design requirements, ensuring the safety and accuracy of the landing process. See Fig.3(b) & Fig.3(c) the V_x & V_y has converge to zero, which means the drones has hovering at the last 5s.

Compared with existing technology, this model provides the obstacle avoidance function and more stable flight attitude of tilt-rotor UAV when it changes from fixed-wing mode to quad-rotor mode at high speed. Github link: <https://github.com/renmingyuhhh/Attitude-Stability-of-tilt-rotor-UAV-during-Obstacle-Avoidance-and-Transition-mode>.

4. Conclusion

In this tilt-rotor UAV high-speed obstacle avoidance and landing test, the UAV showed excellent performance and stability. The high-speed obstacle avoidance and landing test of the tilt-rotor UAV has achieved a complete success. The UAV not only successfully realized the obstacle avoidance function, but also maintained a stable posture during the transition process and landing stage, fully demonstrating its excellent performance and reliability. This achievement not only provides strong support for the further application of tilt-rotor UAV, but also lays a solid foundation for the development of future UAV technology.

References

- [1] Z. Chen and H. Jia, "Design of Flight Control System for a Novel Tilt-Rotor UAV," *Complexity*, vol. 2020, pp. 1–14, Mar. 2020, doi: <https://doi.org/10.1155/2020/4757381>.
- [2] A.C. Daud Filho and E. M. Belo, "A tilt-wing VTOL UAV configuration: Flight dynamics modelling and transition control simulation," *The Aeronautical Journal*, vol. 128, no. 1319, pp. 152–177, May 2023, doi: <https://doi.org/10.1017/aer.2023.34>.
- [3] B. Na, H. Choi, and K. Kong, "Design of a Direct-Driven Linear Actuator for a High-Speed Quadruped Robot, Cheetaroid-I," *IEEE/ASME Transactions on Mechatronics*, vol. 20, no. 2, pp. 924–933, Apr. 2015, doi: <https://doi.org/10.1109/tmech.2014.2326696>.
- [4] Pavan N, "Design of Tiltrotor VTOL and Development of Simulink Environment for Flight Simulation"
- [5] "Docs," *Feishu.cn*, 2024. <https://u0hfx9kgt5s.feishu.cn/docx/Rlf3dZuIOoXvTcxk0VNcA3ZInxh> (accessed Aug. 22, 2024).
- [6] Q. zhang, J. zhang, X. Wang, Y. Xu, and Z. Yu, "Wind Field Disturbance Analysis and Flight Control System Design for a Novel Tilt-Rotor UAV," *Ieee.org*, 2024. <https://ieeexplore.ieee.org/stamp/stamp.jsp?arnumber=9265198> (accessed Aug. 17, 2024).
- [7] Aabid, Abdul & Parveez, Bisma & Parveen, Nagma & Khan, Sher & Raheman, Md Abdul & Zayan, Mohammed & Ahmed, Omar. (2022). Reviews on Design and Development of Unmanned Aerial Vehicle (Drone) for Different Applications. *Journal of Mechanical Engineering Research and Developments*. 45. 53-69.
- [8] T. Lombaerts, J. Kaneshige, S. Schuet, G. H. Hardy, B. L. Aponso, and K. H. Shish, "Nonlinear Dynamic Inversion Based Attitude Control for a hovering quad tiltrotor eVTOL vehicle," *Jan. 2019*, doi: <https://doi.org/10.2514/6.2019-0134>.
- [9] Mehdi Zareb, W. Nouibat, Yasmina Bestaoui, R. Ayad, and Yasser Bouzid, "Evolutionary Autopilot Design Approach for UAV Quadrotor by Using GA," *Iranian Journal of Science and Technology-Transactions of Electrical Engineering*, vol. 44, no. 1, pp. 347–375, Mar. 2020, doi: <https://doi.org/10.1007/s40998-019-00214-6>.
- [10] M. Atmaca, B. Çetin, and E. Yılmaz, "CFD Analysis of Unmanned Aerial Vehicles (UAV) Moving in Flocks," *Acta Physica Polonica A*, vol. 135, no. 4, pp. 694–696, Apr. 2019, doi: <https://doi.org/10.12693/aphyspola.135.694>.
- [11] Jingyi Liu, "Overview of Key Technologies for Tilt-Rotor UAV," *Journal of Aerospace Science and Technology*, vol. 10, no. 04, pp. 99–107, Jan. 2022, doi: <https://doi.org/10.12677/jast.2022.104011>.
- [12] Z. Zuo, C. Liu, Q.-L. Han, and J. Song, "Unmanned Aerial Vehicles: Control Methods and Future Challenges," *IEEE/CAA Journal of Automatica Sinica*, vol. 9, no. 4, pp. 601–614, Apr. 2022, doi: <https://doi.org/10.1109/jas.2022.105410>.
- [13] M. Gemeinder and M. Gerke, "GA-based path planning for mobile robot systems employing an active search algorithm," *Applied Soft Computing*, vol. 3, no. 2, pp. 149–158, Sep. 2003, doi: [https://doi.org/10.1016/s1568-4946\(03\)00010-3](https://doi.org/10.1016/s1568-4946(03)00010-3).